Tubular Web Reduced Beam Section (TW-RBS) connection, a numerical and experimental study and result comparison

Seyed M. Zahrai [1a], Seyed R. Mirghaderi [1b] and Aboozar Saleh [*2]

[1] *School of Civil Engineering, College of Engineering, The University of Tehran, Iran*
[2] *Department of Civil Engineering, Islamic Azad University Professor Hesabi branch, Tafresh, Iran*

Abstract.   A kind of accordion-web RBS connection, "Tubular Web RBS (TW-RBS)" connection is proposed in this research. TW-RBS is made by replacing a part of web with a tube at the desirable location of the beam plastic hinge. This paper presents first a numerical study under cyclic load using ABAQUS finite element software. A test specimen is used for calibration and comparison of numerical results. Obtained results indicated that TW-RBS would reduce contribution of the beam web to the whole moment strength and creates a ductile fuse far from components of the beam-to-column connection. Besides, TW-RBS connection can increase story drift capacity up to 9% in the case of shallow beams which is much more than those stipulated by the current seismic codes. Furthermore, the tubular web like corrugated sheet can improve both the out-of-plane stiffness of the beam longitudinal axis and the flange stability condition due to the smaller width to thickness ratio of the beam flange in the plastic hinge region. Thus, the tubular web in the plastic hinge region improves lateral-torsional buckling stability of the beam as just local buckling of the beam flange at the center of the reduced section was observed during the tests. Also change of direction of strain in arc shape of the tubular web section is smaller than the accordion webs with sharp corners therefore the tubular web provides a better condition in terms of low-cycle fatigue than other accordion web with sharp corners.

Keywords: cyclic behavior; moment resisting steel frames; rigid connection; reduced beam section; Tubular Web RBS (TW-RBS)

1. Introduction

The concentrated tensions and vulnerability of the welded connections to high ductility demands have been considered as the main critical factors of the observed failures in experiences of the Northridge and Kobe earthquakes. The most extensive study has been done by the SAC committee leading to useful results published in the set of FEMA 350 (2000). A common way to resolve this issue is to reduce the ductility demand and related concentrated tensions in these regions. Thus, different techniques have been investigated in order to reduce imposed demands on the beam-to-column connection. Among others, Reduced Beam Section (RBS) moment connection is one of the most economical and practical prequalified connections. RBS connections have been developed by intentionally reducing the plastic capacity of the beam section to make plastic hinge formation at a predefined region along the beam away from the column face.

SAC committee (2000) studied the results of 45 tests on RBS connection after the Northridge Earthquake, during 1996 to 1998. According to their results, the radius cut RBS

connection showed successful behavior and the connection behavior depended on the beam depth. Chen and Chao (2001) examined the effects of concrete slab on moment connection by reduced section and showed that the positive to negative moment capacity ratio can be 1.18 with the presence of slab. Nakashima and Kanao (2002) analytically and numerically studied the lateral torsional instability and lateral bracing effects of wide-flange steel beams subjected to cyclic loading. Jay-Shen *et al*. (2002) showed that the lateral beams and floor slab provide suitable lateral bearing for the beam. Jones *et al*. (2002) experimentally investigated the effects of panel zone, concrete slab and also the effect of the web connection type. Roeder (2002) summarizing SAC committee research expressed that development of shear deformation in panel zone in the RBS connections can also enhance the ductility demand on the column flange weld.

Using balanced panel zone in an analytical and experimental research report, Ricles *et al*. (2004) presented that panel zone in the RBS connections plays an important role in connection behavior. Lee *et al*. (2005) using eight full-scale tests showed that strong panel zone leads to dissipating total energy in the reduced region. Moslehi Tabar and Deylami (2005) numerically studied the instability of RBS connection concentrating on the effect of plasticity shear panel in columns. Their results indicated that not only the rigid shear panel keeps the panel zone in the elastic range but it also causes instability of the beam cyclic behavior. Zhang and Ricles (2006a, b) demonstrated

*Corresponding author, Assistant Professor,
  E-mail: aboozar.saleh@ut.ac.ir
[a] Professor, E-mail: mzahrai@ut.ac.ir
[b] Associate Professor, E-mail: rmirghaderi@ut.ac.ir

that concrete floor supports beam top flange increasing the ultimate load in the plastic hinge which is not included in design procedures. Han and Moon (2009) showed that if the span to depth ratio is less than 10 and if the beam flange bending moment contribution is less than 70% of the beam flexural strength, using web bolted connection is not recommended. Pachoumis *et al*. (2010) studied cyclic behavior of RBS moment connections through experimental and numerical analyses. They showed that using the RBS connection in European sections requires changing the RBS geometric parameters.

Connection with web reduction is another type of reduced beam section connections. For example, Rao and Kumar (2006) studied a connection with rectangular hollow in web, entitled Rectangular Hollow Sections (RHS). Behavior of RBS connections with web circular holes has been investigated by Yang and Yang (2009). Behavior of beams with perforated webs has been also studied by Tsavdaridis and D'Melloon (2012). They have focused on beams with elliptical web opening and concluded that such details can lead to satisfactory results both in terms of technical and constructional points of view.

Most conventional RBS connections and those with web reduction would reduce out-of-plane stiffness of the beam and are vulnerable to lateral-torsional buckling. To resolve this problem Wilkinson *et al*. (2006) have evaluated a new detail by which the web height reduction near the connection of beam-to-column was achieved. The experimental results approved plastic rotation capacity of more than 5%. Mirghaderi *et al*. (2010) discussed and evaluated bending beam connection of reduced cross section by corrugated web in an experimental and analytical study. Two symmetric angles were considered in two test samples with respect to the web as corrugated sheet to execute removed web accommodation and create a cross section as accordion web RBS (AW-RBS). The results of both tests were correlated without strength degradation up to 8% story drift. Morrison *et al*. (2015) experimentally studied an innovative technique for reduced flexural capacity. The technique involves strength reduction of specified regions of the beam flanges by exposing them to high temperatures followed by slow cooling. Analogous to the RBS connection, yielding and plastic hinge formation is promoted in the Heat-treated Beam Section (HBS). The results showed that HBS connection experienced story drifts as high as 6% without any weld or near weld fracture.

Parallel to the connection with accordion web, in this paper a new web RBS connection called "TW-RBS" is proposed for steel moment resisting frames. In the proposed connection, the beam section is reduced using a pipe instead of a flat web at the expected location of the beam plastic hinge in the vicinity of the beam–to–column connection. The tubular web provides even a better condition than AW-RBS connection in low-cycle fatigue, by changing sharp corners of angles to arc shape of the tubular web section. In this regard, the present study aims to numerically and experimentally investigate the seismic behavior and cyclic response of the new proposed connection.

2. Proposed connection: TW-RBS

2.1 Behavior of corrugated web

The flexural behavior of beam with corrugated web considerably differs from a flat web. This different behavior is derived from the difference between the nature of the flat and corrugated sheets. Flat sheet in the in-plane stress has an isotropic behavior, while stiffness of corrugated sheet in *x* and *y* directions are completely different.

In the longitudinal direction, stiffness is sharply reduced. This small stiffness in corrugated sheet causing deformation under load is similar to opening and closing accordion. This behavior is called accordion behavior. So by using accordion web in beam due to the lack of strain in the web and thereby little participation of corrugated web in flexure resistance, the ultimate bending capacity can be determined only based on the beam flange plastic capacity while web effect can be ignored. In this case, the whole shear is mainly tolerated by the corrugated web. Previous studies have also shown that there is no interaction between the flexural behavior and shear behavior of beams with corrugated web (Elgaaly *et al*. 1997a, b).

2.2 Determining the appropriate location of the TW-RBS

Connection design approach is based on AISC seismic provisions (2010). In order to reduce demand and decrease the failure of beam welded to column connection and surrounding material, the maximum moment demand at the column face must be lower than the nominal plastic strength in that specific point. Therefore, as illustrated in Fig. 1, the maximum moment generated at the column face (M_f) can be obtained from the image of the maximum expected moment established in the center of the reduced beam section ($M_{TW\text{-}RBS}$) as follows
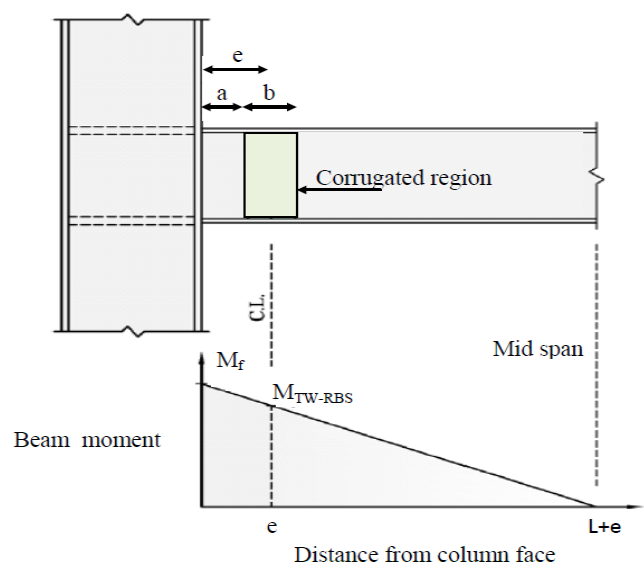

Fig. 1 Bending moment gradient for seismic loading

$$M_f = M_{TW-RBS} \frac{(L+e)}{L} \qquad (1)$$

Where, L is the distance between the centerline of reduced beam section to middle span. Compared to the seismic demand, the gravity load on the beam is assumed small then the moment distribution is linear. Maximum expected moment created in the center of reduced beam section (M_{TW-RBS}) based on seismic criteria is defined as follows

$$M_{(TW-RBS)} = 1.1 R_y Z_{(TW-RBS)} F_y \qquad (2)$$

Where Z_{AW-RBS} is the plastic section modulus of the corrugated region and R_y is the ratio of the expected yield stress to the minimum specified yield stress (F_y). Maximum moment demand at the column face ratio to the nominal plastic strength is calculated as follows

$$\alpha = \frac{M_f}{Z_b R_y F_y} = \frac{M_{(TW-RBS)} \frac{(L+e)}{L}}{Z_b R_y F_y}$$
$$= \frac{1.1 R_y Z_{(TW-RBS)} F_y \frac{(L+e)}{L}}{Z_b R_y F_y} = \frac{1.1 Z_{(TW-RBS)}(L+e)}{Z_b L} \qquad (3)$$

In the equation above, Z_b is plastic modulus in unreduced beam section, at the column face. In order to reduce demand and failure risk in welded connection of beam and the column face, the value of α must be lower than 1. The recommended value for this parameter in design of common reduced beams is 0.9 (Engelhardt *et al.* 1998). Therefore, the plastic modulus of reduced and unreduced beam section and the length of cantilevered beam ($L + e$) determine the appropriate distance from the center of reduced section to the column face.

3. Finite element modeling

3.1 Subassembly and the selected dimensional parameters

The proposed subassembly used in similar experimental studies investigated by Mirghaderi *et al.* (2010) was chosen to confirm the AW-RBS connection behavior. It consisted of an interior connection with beams attached to the column opposite faces. In this subassembly, half of the parts of lower and upper columns was chosen as vertical element and half of the beam was chosen for horizontal element.

For modeling the connection, box-column (built-up 200×160×10) and IPE180 are chosen respectively for column and beam as shown in Table 1. The geometrical

Table 1 Determining the beam and column specifications

Section	A_b (m^2×10^{-4})	d_b (m×10^{-2})	b_f (m×10^{-2})	t_f (m×10^{-2})	t_w (m×10^{-2})
IPE180	23.9	18	9.1	0.8	0.53
Box200×160×10	64.0	18	14	1.0	1.0

* Cross-section Area: A_b; Depth of section: d_b
Width and Thickness of flange: b_f and t_f; Thickness of web: t_w

dimensions are 2150 mm for the vertical members, acting as the columns, and 3290 mm (distance between the rollers boundary condition of two beams) for the horizontal members, behaving as the beams. The selected sections satisfy width-thickness ratio of seismically compact section. Also this geometry of element models, including member section sizes and all dimension and boundary conditions, are considered as per the subassembly used in the experimental program in this research.

The distance of center of tube to the column face, and also diameter of tube, are obtained from the Table 2 and Eq. (4).

As it can be observed, with considering the allowed range for e, the diameter of tube can be determined from Eq. (4)

$$D = 2(e - a) \qquad (4)$$

So by letting $a = 5.35$, it gives a value of 7.3 cm for tube outside diameter. The thickness of available steel pipe in the market according to DIN-2440, is 5.5 mm, which is known with nominal diameter of 65 mm (2-1/2 inch).

According to the reduced section plastic modulus, the expected moment is specified in the beam plastic hinge location and the condition of weak beam-strong column is controlled, as presented in Table 3 in which expected yielding stress of material ($F_{ye} = R_y F_y = 1.5 \times 2400 = 3600$) has been used. Sufficient safety factor for column face demand is provided ($\alpha = 0.925$).

Beam shear must be controlled in the plastic hinge (according to Appendix 2) along tubular web and its outside. The proposed connection established required beam shear.

Minimum thickness of shear panel was obtained from Eq. (5)

$$t_z \geq \frac{w_z + d_z}{90} \qquad (5)$$

In Eq. (5), w_z and d_z are the width and depth of panel zone respectively; so by substituting 18 and 18 cm in Eq. (5), the minimum thickness of the panel zone is 0.4 cm. This control criterion is established according to thickness

Table 2 Determining reduced section dimensional parameters

Section	Z_b (m^3×10^{-6})	$Z_{TW-RBS*}$ (m^3×10^{-6})	$L+e$ (m×10^{-2})	e (m×10^{-2})	Allowed range of e $0.5d_b < e < d_b$ (m×10^{-2})	Allowed range of a $0.5b_f < a < 0.75b_f$ (m×10^{-2})
IPE180	166	131.44	154.5	9	9 < e < 18	4.55 < a < 6.83

* Plastic modulus of unreduced section: Z_b; Plastic modulus of reduced section: Z_{TW-RBS} (Appendix 1);
Length of beam: $L+e$;   Distance from the center of reduced section to the column face: e (Eq. (3))

Table 3 Beam design check at the column face

$Z_{TW\text{-}RBS}$ $(m^3 \times 10^{-6})$	$M_{TW\text{-}RBS}$ (kN-m)	L $(m \times 10^{-2})$	e $(m \times 10^{-2})$	M_f (kN-m)	$Z_b F_{ye}$ (kN-m)	α	$e + d_c/2$ $(m \times 10^{-2})$	$\sum M_{pb}$ (kN-m)	$\sum M_{pc}$ (kN-m)	$\sum M_{pc}/\sum M_{pb}$
131.44	52.05	145.5	9	55.27	59.76	0.925	19	117.7	205.44	1.75

* Expected moment in plastic hinge location: $M_{TW\text{-}RBS}$; Beam moment at the column face location: M_f
  Moment ratio at the column face: $\alpha = M_f / Z_b F_{ye}$; Beam moment in center of column: $\sum M_{pb} = M_f$;
  Column plastic moment: $\sum M_{pc} = \sum Z_c F_{yc}$
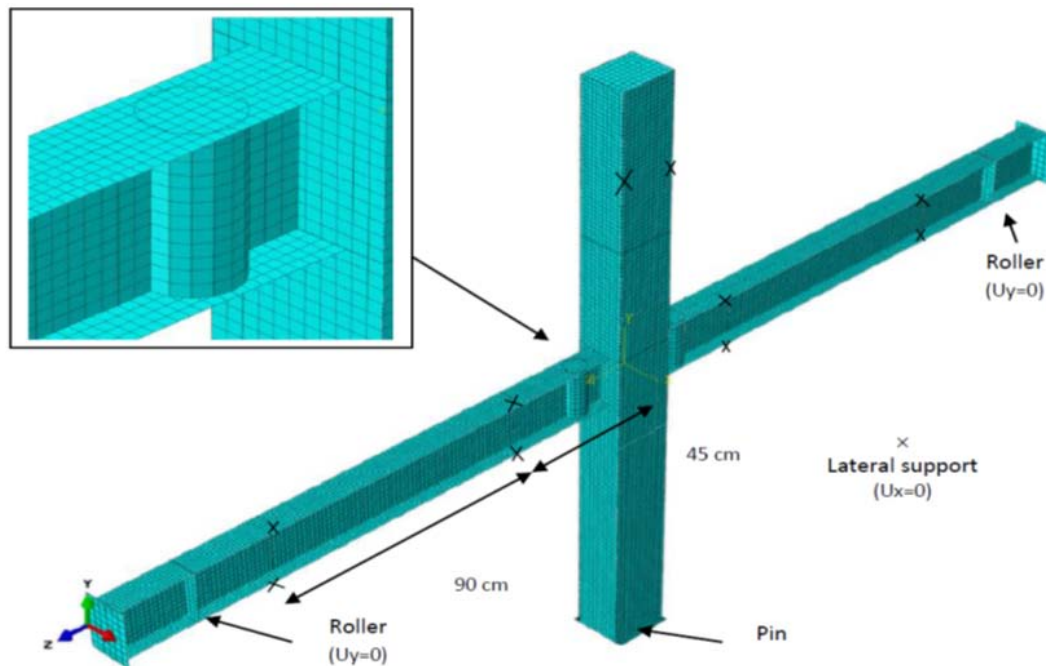
(a) Finite elements mesh
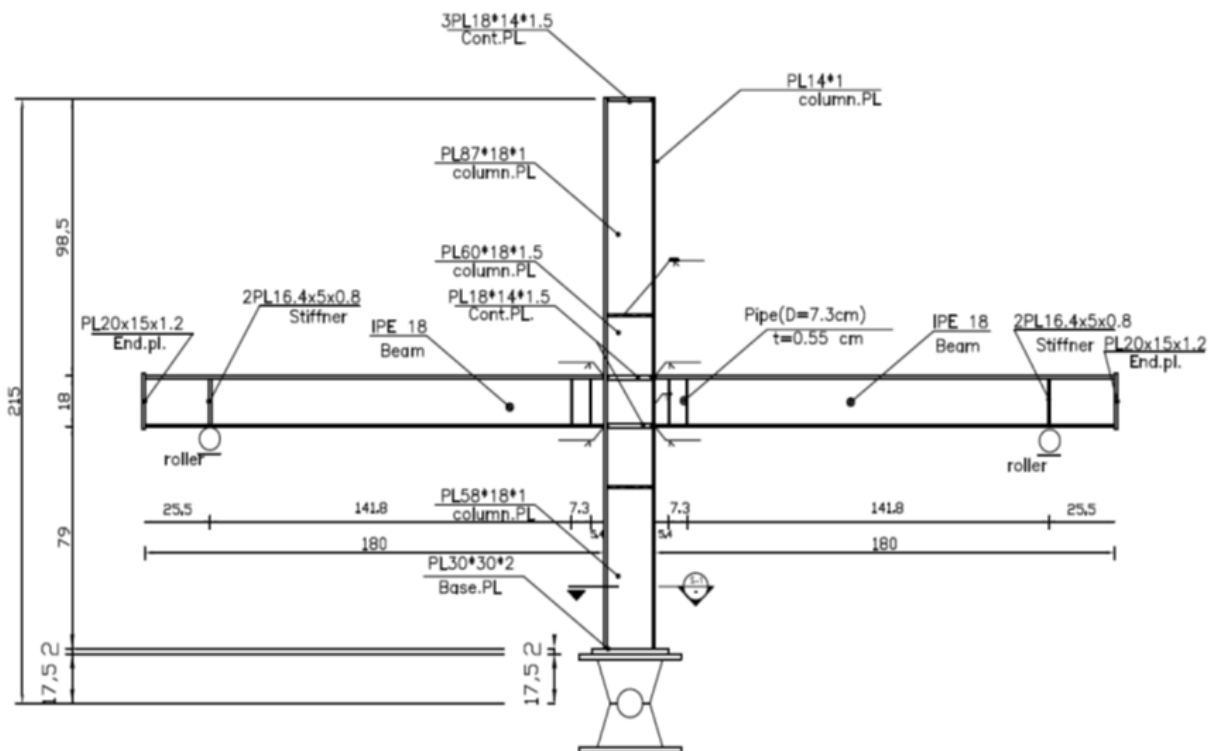
(b) Geometry of proposed connection

Fig. 2 Finite element modeling for the proposed TW-RBS connection

of box-column.

Continuity plates of $180 \times 140 \times 15$ mm^3 were used in the panel zone. This sheet not only tolerates the imposed tensile and compressive force from the beam flange but also conversely converts the axial force to shear force in panel zone, since the established length to width ratio is greater than 1.5 on this sheet. In addition, width to thickness ratio in $b/t < 800/\sqrt{F_y}$ is also satisfied. Thus, the proposed model is already defined and can be simulated with ABAQUS software.

3.2 Description of meshing components

Numerical analysis is carried out using a three-dimensional finite element model in ABAQUS (1997). The geometry of finite element models, including member section sizes and all dimension and boundary conditions,

Table 4 Mechanical properties of steel coupons

Member	Coupon	Yield strength (MPa)	Tensile strength (MPa)	Elongation (%)
Beam	Flange	325	489	26
Beam	Web	328	468	33
Pipe	-	649	744	22
Box-column	Web & Flange Plates	266	400	44
Box-Column	Panel zone & continuity plates	283	407	45.5

are considered as Section 3.1, same as the subassembly used in the experimental program in this paper as shown in Fig. 2. Given the assumption of the SHELL behavior of components in this model, deformable SHELL is defined for all components. Four-node tetrahedral element with six degrees of freedom (three translational degrees and three rotational degrees) was used for meshing the components. Mesh size of all components is similar (maximum dimension 1.5 cm) except for beam flange (maximum dimension 1.25 cm). All regarded elements are square-shaped and degrees of freedom in connection zone are bound together with Tie constraints.

3.3 Material properties

Due to the fact that materials are supposed to exceed their linear range, the analysis should be done considering nonlinear behavior. The kinematic hardening was selected for plastic properties, the yield strength (F_y) and the ultimate strength (F_u) and also the plastic strain of the materials are considered as per the tensile coupon test results, as summarized in Table 4. The Young modulus of elasticity and Poisson ratio are assumed as 203 GPa and 0.3, respectively, for all materials of the analysis. Bilinear behavior curve was used to define the mechanical properties, where the slope of the elastic behavior is Young modulus of elasticity and the slope nonlinear behavior is obtained from connecting the yield point (ε_y, F_y) to the failure point (ε_u, F_u) on stress–strain curve.
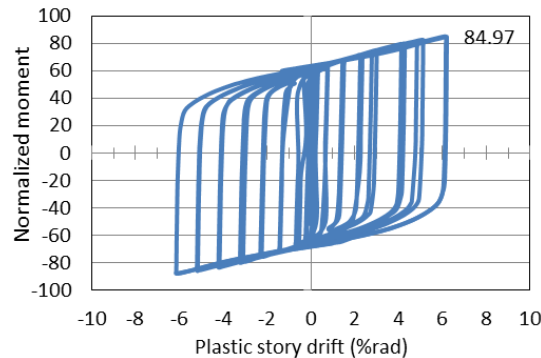
3.4 Definition of load type and analysis
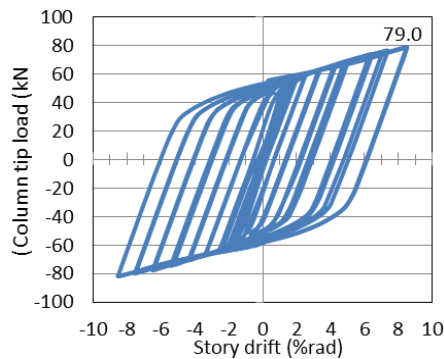
(a) Column tip Force versus story drift
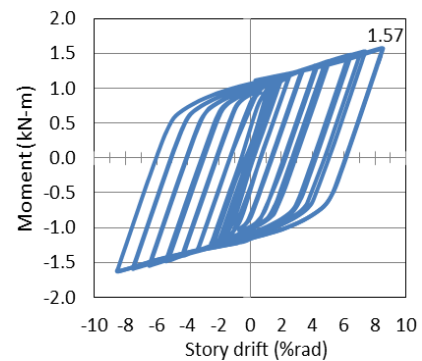
(b) Moment of beam at the column face versus story drift

(c) Normalized moment of beam at the column face versus plastic story drift

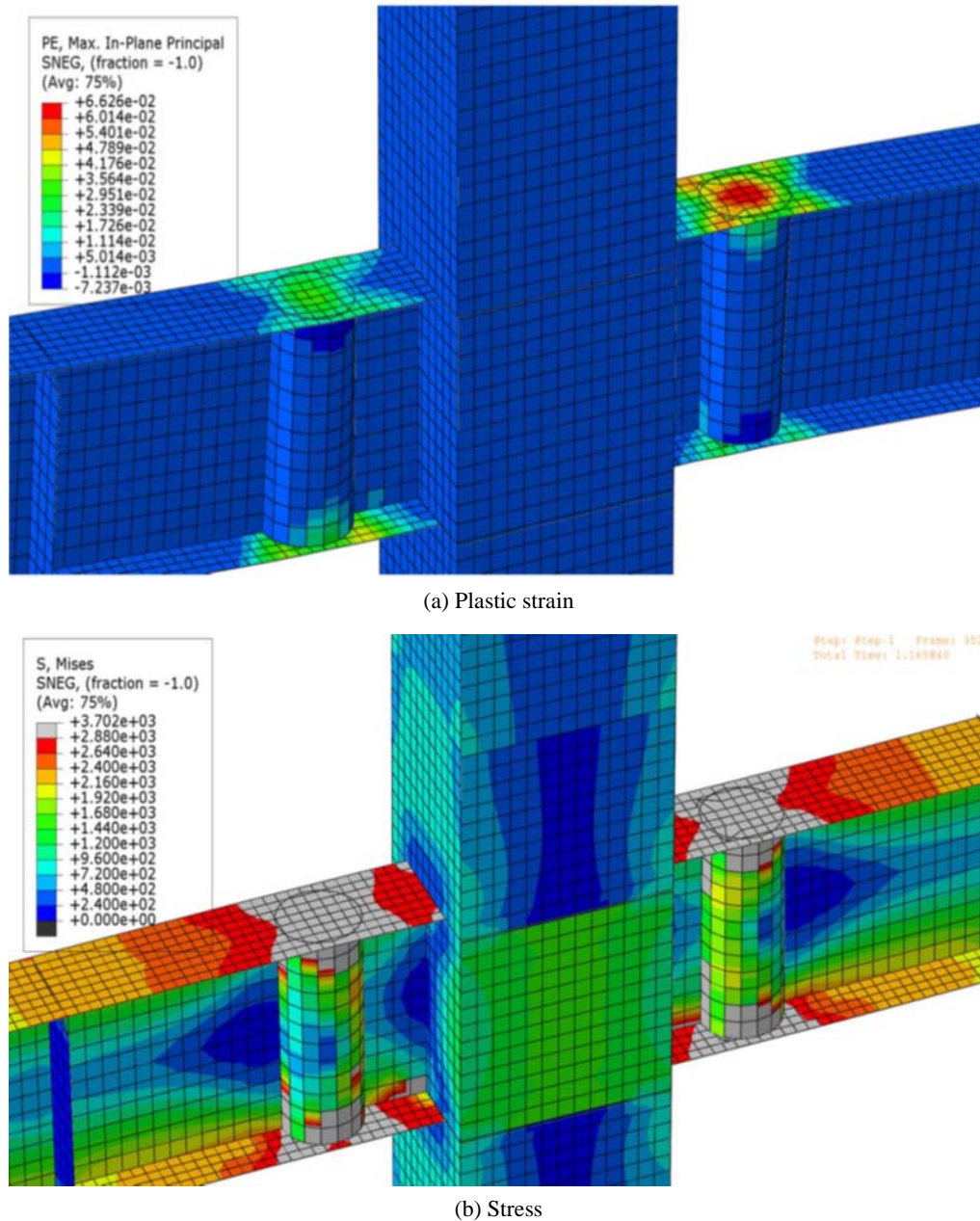Fig. 3 Numerical results of the proposed model

(a) Plastic strain

(b) Stress

Fig. 4 Von-Mises stress and strain contours at 0.06 radian story drift

The standard solver of ABAQUS software (ABAQUS/ Standard) was used for analyzing the model. In load section, supports were defined by setting up boundary conditions. Furthermore, cyclic loading was imposed on the structure by defining boundary conditions as a displacement on top of the column based on AISC Seismic Provisions (2010). The model investigated by ABAQUS was loaded to reach 9% story drift. Thus, at each drift of 0.00375, 0.005 and 0.0075 radians 6 cycles, at 0.01 radians drift 4-cycles and finally at drift of 0.015, 0.02, and 0.03 to 0.08 radians, two cycles were respectively considered.

Boundary condition for bottom of the column was defined by fixing degree of freedom in 3 directions. Roller support was defined at the distance of 154.5 cm from the column face by fixing degree of freedom in vertical direction. To define lateral support, out-of-plane displace-

ment of beam web was fixed at 45 and 135 cm from the side of the column. Also the column was fixed with a lateral support in its upper half.

4. Numerical results

4.1 Numerical results

Lateral force-story drift cyclic curve is presented in Fig. 3(a) for the proposed connection. The drift is obtained from dividing lateral displacement at top of column to the column height. Also Fig. 3(b) provides the story drift-moment curve of beam at the column face. The moment at the column face is calculated through equilibrium in sub-structure. Increasing demand on these curves is due to

entering material in strain hardening area.

Plastic story drift versus normalized moment curve at the column face is also presented in Fig. 3(c). Plastic story drift is obtained by subtracting the elastic story drift from the total story drift. The moment at the column face is normalized to beam nominal flexural capacity until the additional resistance of structures is estimated.

The results of the proposed model satisfy AISC seismic provisions (2010) acceptance criteria to confirm that special moment frame connection tolerates at least 0.03 radian story drift and, the flexural capacity of the specimen at the column face should not be less than 80% of the beam plastic moment at 0.04 radian story drift. The proposed connection provides a stable cyclic behavior without strength reduction up to 9% story drift.

The Von-Mises stress and strain contours at 0.06 radian story drift are illustrated in Fig. 4 for both positive and negative bending moments. The stress is shown by units of kg/cm². Gray color represents the yielding area and tension contour shows formation of plastic hinge in the center of

corrugated area. Flange tension near the column face is lower than that in the place of plastic hinge formation. Studying the tension distribution in the corrugated web indicates that the value of tension in corrugated web is much lower than that in beam flange.

The results show that the hinge is formed at the accordion area; and the plastic strain in the surrounding corrugated area has far less intensity while the rest of area remains elastic. This reduction in strain demand at the column face and full penetration welds in beam-to-column connection significantly reduces risk of failure at the full penetration welds.

4.2 Result verification

Numerical studies alone may not be sufficient to support the TW-RBS connection. Cyclic plastic deformation, low cycle fatigue endurance and the behavior of the welds without cyclic tests are unknown on TW-RBS connection. Then for validation/calibration purposes of the numerical model, experimental program has been carried out to study

(a) Test result

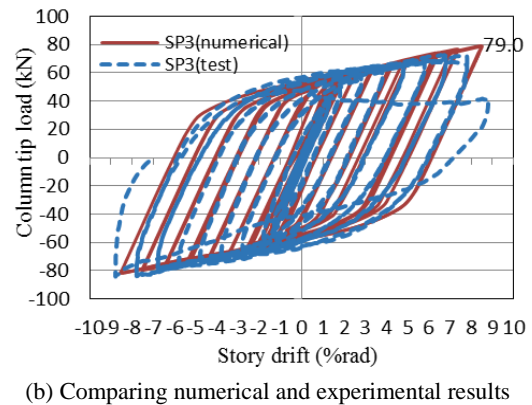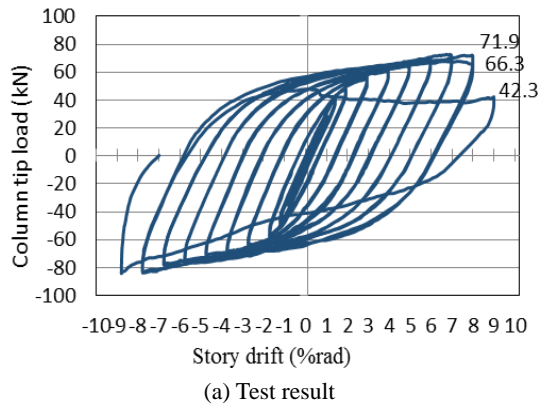(b) Comparing numerical and experimental results

Fig. 5 Column tip Force versus story drift for TW-RBS specimen

(a) First yielding at the center of the reduced region at 1.5% story drift

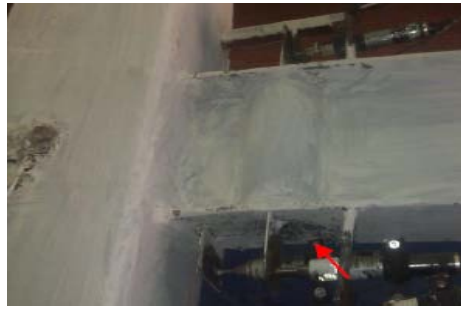(b) The extension of the yielding at 2% story drift

(c) The extension of the yielding at 3% story drift

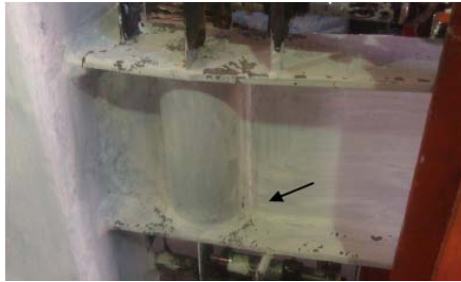(d) Local buckling in the right beam at 4% story drift

Fig. 6 TW-RBS experimental results up to 4% story drift

(a) Local buckling at 5% story drift

(b) Local buckling at 5% story drift

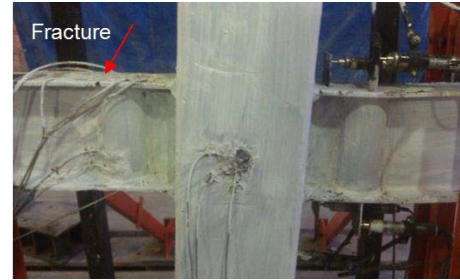(c) Yielding at the tubular web at 5% story drift

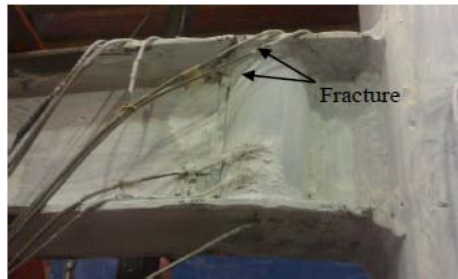(d) Local buckling at 6% story drift

Fig. 7 TW-RBS experimental results at 5 and 6% story drifts
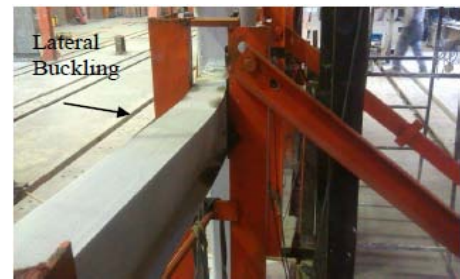

(a) Lateral-torsional buckling in the left beam at 7% story drift

(b) Fracture in the left beam at 8% story drift

(c) The crack spread at the second cycle of 8% story drift

(d) Lateral buckling at 8% story drift

Fig. 8 TW-RBS experimental results at 7 and 8% story drifts

the behavior of TW-RBS moment connections. All dimensions and design of connection are according to what already mentioned for numerical model. Lateral force-story drift cyclic curve of experimental results compared to that of numerical results is presented in Fig. 5 for TW-RBS. As shown in Fig. 5, TW-RBS test specimen provides a stable cyclic behavior without strength reduction up to 8% story drift satisfying AISC seismic provisions (2010) and FEMA (2000) acceptance criteria up to 9% story drift, also validating the numerical model.

According to the test observations, first yielding emerged on the beam flanges at the center of the reduced region during the first cycle of 1.5% story drift cycles as shown in Fig. 6(a). It was spread over the entire reduced region and extended toward the column face and beam end during next story drifts (Fig. 6(b)-(c)). Flange local buckling was detected in the reduced region in both sides of beam following to the 4% story drift as shown in Fig. 6(d).

The amplitude of flange local buckling increased at the 5% story drifts as shown in Fig. 7(a)-(b). In the 6% drift,

the yielding at the tubular web extended into the beam depth (Fig. 7(c)) and the amplitude of flange local buckling increased again (Fig. 7(d)).

In the first cycle of 7% story drift, lateral-torsional buckling of beam appeared in the top flange of left beam, immediately after the reduced region as shown in Fig. 8(a). The amplitude of lateral-torsional buckling of beam increased in the second cycle of 7% story drift. In the first cycle of 8% story drift, the crack was initiated in the top flange of left beam immediately after the reduced region as shown in Fig. 8(b). The crack progressed to the middle of flange and fracture was initiated in the connection weld of tubular web to flat web at this part, during the second cycle of 8% story drift as shown in Fig. 8(c). The lateral-torsional buckling of the beams is shown in this story drift as observed in Fig. 8(d).
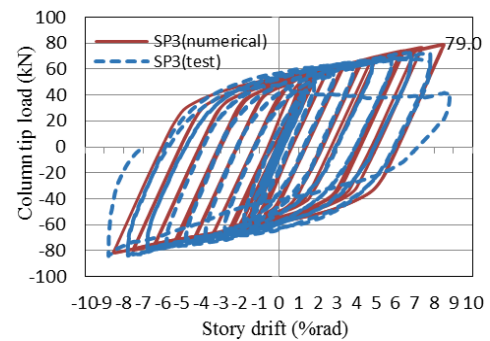
The cracks progressed down into connection of the tubular web to flat web during the first cycle of 9% story drift as shown in Fig. 9(a). At the following second half of first cycle of 9% story drift, the cracks and rupture were initiated in the bottom flange of right beam, exactly in the reduced region as shown in Fig. 9(b). According to the test, low cycle fatigue cannot happen at tubular webs and lateral-torsional buckling stability would be maintained up to high story drifts.

5. Result comparison

Numerical results of TW-RBS connection are compared
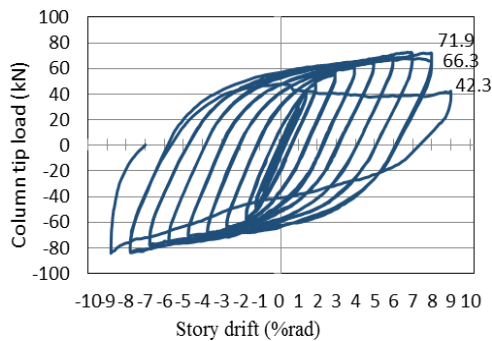
to experimental counterparts at this section. According to the results, local buckling of compression flange at reduced section in TW-RBS has occurred at 4% story drift. The TW-RBS connection satisfies AISC seismic provisions (2010) and FEMA-350 (2000) acceptance criteria up to 9% story drift.

In Fig. 10, numerical and experimental results of normalized strains ($\varepsilon/\varepsilon_y$) at the width of the beam flange at the center of the reduced region (9 cm from column face) are presented. According to the limitation of the number of strain gauge in experimental model (two strain gauges at the width of the beam flange), numerical results are used with more points to better understand the strain distribution. The development of the plastic hinge in the predefined region is confirmed by higher values of normalized strain at the center of reduced region.

The numerical results in Fig. 10, show that the distribution is not uniform, i.e., at the center of the reduced region and near area have a high strain level but away from the center, the strain level drops. This would justify that the contact point of beam flange to the tubular web is a turning point of the strain distribution curve.

Numerical and experimental normalized strain curve on different parts of tubular web in TW-RBS is presented in Fig. 11 in order to study the effects of accordion web. As clearly shown, strain profile in corrugated web has a significant decrease in all points in comparison with linear profile of strain distribution in beam web and the accordion web behavior has caused great reduction of the axial strain of beam web at plastic hinge location. According to the
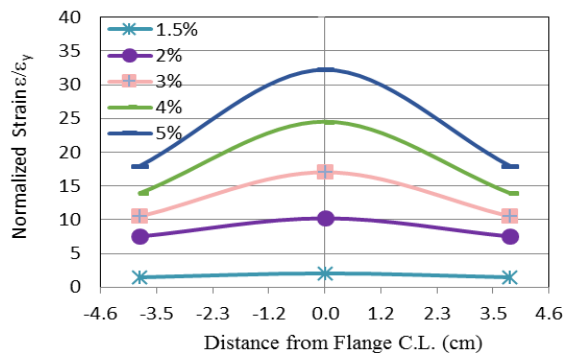

(a) Fracture in the left beam at 9% story drift
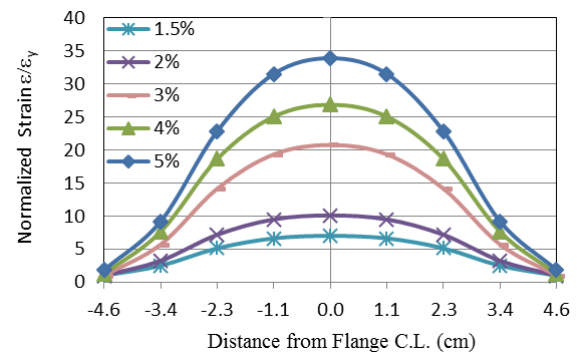

(b) Fracture in the right beam at 9% story drift

Fig. 9 TW-RBS experimental results at 9% story drift

(a) Experimental result

(b) Numerical result

Fig. 10 Envelope of normalized strain ($\varepsilon/\varepsilon_y$) at the width of the beam flange at the center of the reduced region

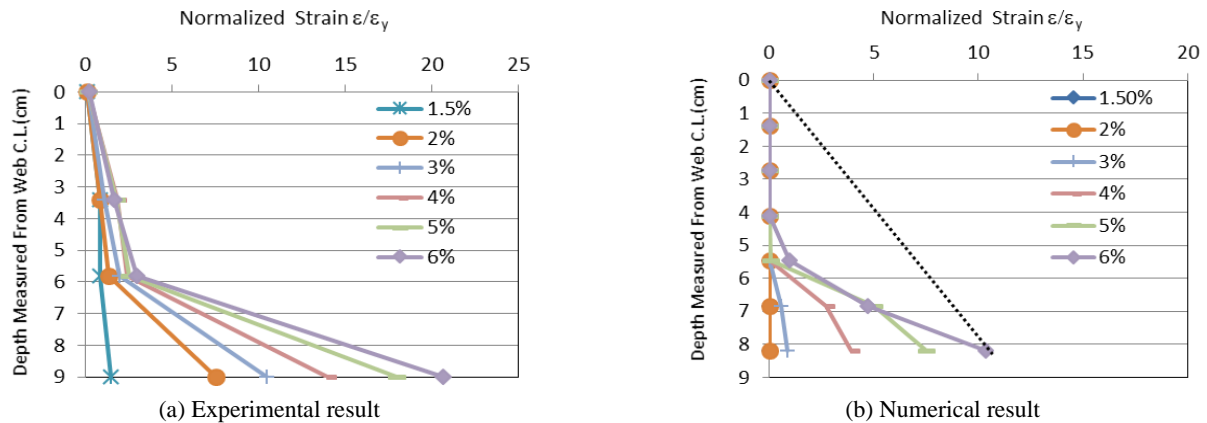(a) Experimental result   (b) Numerical result

Fig. 11 Envelope of normalized strain in tubular web at different distances from the neutral axis

curves, axial strain in the tubular web was increased close to the beam flange; while by taking distance from beam flange, the longitudinal strain of the web was highly decreased and became negligible. The absence of web in the flexural strain leads to elimination of web participation in flexural capacity.

Also according to the results, the tubular web can be divided into three parts on each side of the neutral axis of the beam. A part is at near the neutral axis with minimal strain close to zero. A middle part with low axial strain and a part close to the beam flange with a high axial strain.

Longitudinal strain profiles along the beam tensile and compressive flanges are shown at different story drifts in Fig. 12 by numerical study. Comparing the values of tensile and compressive strain shows that the tensile strain is more than compressive strain in the same story drift. The cause of this phenomenon can be found in the different behavior of materials in the plastic behavior range in tension and compression, because the neutral axis of the beam section is shifted toward compression flange in plastic behavior and farther from tensile flange such that the tensile strains would be more.

Mirghaderi *et al*. (2010) used three connections for making a comparison in numerical study: a usual RBS connection with circular cutting of flange and a rigid beam (IPE180) to column connection and AW-RBS specimen. In
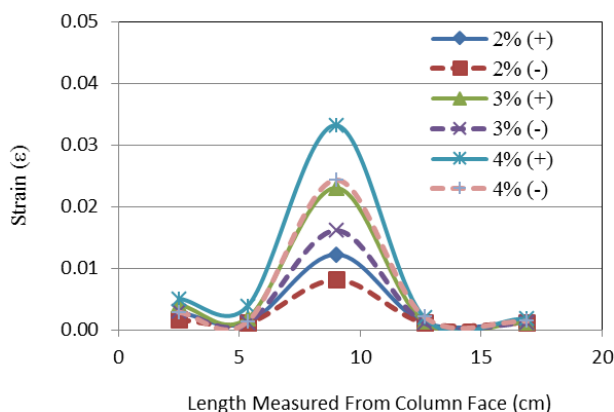
RBS connection, a circular cut of connection begins from 6.75 cm at the column face and the cutting length is 15 cm. The highest reduction in flange width in reduced section is 35%. In the rigid connection, there is no particular design and just the panel zone and continuity plates have been controlled. In a similar numerical study, the normalized moment curves at the column face, $M_f/Z_b F_{ye}$, versus different story drift values in TW-RBS are shown, in Fig. 13.

According to the results, both models of AW-RBS and TW-RBS have lower level of strength compared to rigid connection. At the beginning of yielding, TW-RBS connection demonstrated a lower amount of reduction in strength in comparison with other reduced sections.

The drop of strength on usual RBS and rigid connection shows occurrence of buckling and instability in these connections while the accordion web connection does not experience a significant drop in strength due to the stabilizing factors in plastic hinge zone. AW-RBS demonstrates more hardening after the yielding; thus strength increases with higher rate. The reason is related to the material behavior at this level of strain that a tri-linear stress-strain curve was used in AW-RBS, so that after the yielding strain, the linear diagram of ultimate stress with stiffness of 0.03E would lead to creation of the perfect plastic behavior after 0.0225 strain level. Thus all plastic strain hardenings at the start of yielding are the same as the numerically obtained strain range representing a hardening behavior with greater slopes. However, material behavior in

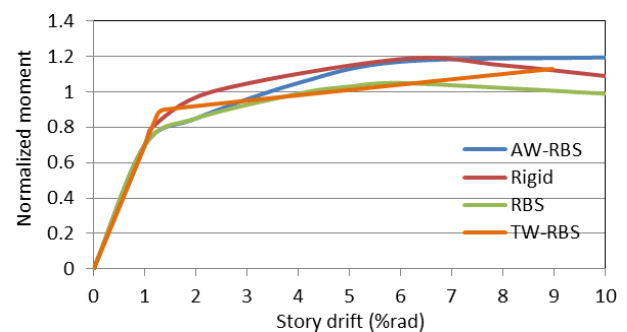Fig. 12 Longitudinal strain profile along the beam top and bottom flange in numerical study

Fig. 13 Normalized moment diagram at the column face versus story drift

the proposed model is bilinear; and the plastic strain hardening is distributed between the ultimate and yielding strains; hence showing a less hardening slope.

6. Conclusions

In this study, a new type of RBS connection, called TW-RBS, was proposed for typical shallow beams and its hysteretic behavior was evaluated experimentally and numerically. TW-RBS has been made through cutting continuous web and replacing that part with a tube at the desired location of the plastic hinge. Overall, the numerical and experimental results demonstrated that the plastic hinge capacity can only be estimated in the reduced region based on the beam flanges and the contribution of the beam web to the plastic hinge capacity is negligible because of the web accordion behavior. Also due to flexural strength reduction by replacing web in proposed connection, using TW-RBS reduces the plastic strain demand near the critical CJP welds and effectively concentrates the plastic strains within the reduced region. Flange local buckling was detected inside the reduced region and lateral-torsional buckling appeared only at a high story drift (7%) in the TW-RBS connection in shallow beams showing an improvement in the out-of-plane stiffness and stability condition of plastic hinge. It is noteworthy that TW-RBS satisfies AISC seismic provisions (2010) and FEMA350 (2000) acceptance criteria up to 9% story drift for the shallow beams studied in this paper.

Acknowledgments

References

American Institute of Steel Construction (2010), AISC, Seismic Provisions for Structural Steel Buildings, Chicago, IL, USA.

Chen, S.J. and Chao, Y.C. (2001), "Effect of composite action on seismic performance of steel moment connections with reduced beam sections", *J. Constr. Steel Res.*, **57**(4), 417-434.

Eldib, M.E. (2004), "Buckling analysis of beams with corrugated webs", *Proceeding of 5th International Conference on Civil and Architecture Engineering (ICCAE Conference)*, Manila, Philippines, March.

Eldib, M.E. (2009), "Shear buckling strength and design of curved corrugated steel webs for ridges", *J. Constr. Steel Res.*, **65**(12), 2129-2139.

Elgaaly, M., Hamlton, R. and Seshadri, A. (1997a), "Shear strength of beams with corrugated webs", *J. Struct. Eng.*, **122**(4), 390-398.

Elgaaly, M., Seshadri, A. and Hamlton, R. (1997b), "Bending strength of steel beams with corrugated webs", *J. Struct. Eng.*, **123**(6), 772-782.

Engelhardt, M., Winneberger, T., Zekany, A. and Potyraj, T. (1998), "Experimental investigation of Dogbone moment connections", *Eng J AISC*, Fourth Quarter, 128-139.

FEMA-350 (2000), Seismic design criteria for new moment resisting steel frame construction, Washington DC, USA.

FEMA-351 (2000), Recommended seismic evaluation and

upgrade criteria for exiting welded steel moment- frame buildings, Washington DC, USA.

FEMA-352 (2000), Recommended posearthquake evaluation and repair criteria for welded steel moment- frame buildings, Washington DC, USA.

FEMA-355D (2000), State of the art report on connection performance, Washington DC, USA.

FEMA-355E (2000), State of the art report on past performance of steal moment- frame buildings in earthquake, Washington DC, USA.

FEMA-355F (2000), State of the art report on performance prediction and evaluation of steal moment frame buildings, Washington DC, USA.

Hamilton, RW. (1993), "Behavior of welded girder with corrugated webs", Ph.D. Dissertation; University of Maine, ME, USA.

Han, S.W. and Moon, H.H. (2009), "Design equations for moment strength of RBS-B connection", *J. Constr. Steel Res.*, **65**(5), 1087-1095.

Jay-Shen, J.H., Astaneh-Asl, A. and McCallen, D. (2002), "Use of deep columns in special steel moment frames", *Steel Tips*, AISC.

Jones, S.L., Fry, G.T. and Engelhardt, M.D. (2002), "Experimental evaluation of cyclically loaded reduced beam section moment connections", *J. Struct. Eng.*, **128**(4), 441-451.

Lee, C.H., Jeon, S.W., Kim, J.H. and Uang, C.M. (2005), "Effect of panel zone strength and beam web connection method on seismic performance of reduced beam section steel moment connection", *J. Struct. Eng.*, **131**(12), 1854-1865.

Mirghaderi, S.R., Torabian, S. and Imanpour, A. (2010), "Seismic performance of the Accordion-Web RBS connection", *J. Constr. Steel Res.*, **66**(2), 277-288.

Morrison, M., Schweizer, D. and Hassan, T. (2015), "An innovative seismic performance enhancement technique for steel building moment resisting connections", *J. Constr. Steel Res.*, **109**, 34-46.

Moslehi Tabar, A. and Deylami, A. (2005), "Instability of beams with reduced beam section moment connections emphasizing the effect of column panel zone ductility", *J. Constr. Steel Res.*, **61**(11), 1475-1491.

Nakashima, M. and Kanao, I. (2002), "Lateral instability and lateral bracing of steel beams subjected to cyclic loading", *J. Struct. Eng.*, **128**(10), 1308-1316.

Pachoumis, D.T., Galoussis, E.G., Kalfas, C.N. and Efthimiou, I.Z. (2010), "Cyclic performance of steel moment-resisting connections with reduced beam sections-experimental analysis and finite element model simulation", *Eng. Struct.*, **32**(9), 2683-2692.

Rao, D.P. and Kumar, S.S. (2006), "RHS beam-to-column connection with web opening—parametric study and design guidelines", *J. Constr. Steel Res.*, **62**(8), 747-756.

Ricles, J.M., Zhang, X., Lu, L.W. and Fisher, J.W. (2004), "Development of seismic guidelines for deep column steel moment connections", ATLSS Report No 04-13.

Roeder, C.W. (2002), "Connection performance for seismic design of steel moment frames", *J. Struct. Eng.*, **128**(4), 517-525.

Tsavdaridis K.D. and D'Mello C. (2012), "Optimisation of novel elliptically-based web opening shapes of perforated steel beams", *J. Constr. Steel Res.*, **76**, 39-53.

Wilkinson, S., Hurdman, G. and Crouther, A. (2006), "A moment resisting connection for earthquake resisting structure", *J. Constr. Steel Res.*, **62**(3), 295-302.

Yang, Q. and Yang, N. (2009), "Seismic behaviors of steel moment resisting frames with opening in beam web", *J. Constr. Steel Res.*, **65**(6), 1323-1336.

Zhang, X. and Ricles, J.M. (2006a), "Experimental evaluation of reduced beam section connections to deep columns", *J. Struct. Eng.*, **132**(3), 346-357.

Zhang, X. and Ricles, J.M. (2006b), "Seismic behavior of reduced
    beam section moment connections to deep columns", *J. Struct.
    Eng.*, **132**(3), 358-367.

BU

Appendix 1
Assessment of resistance mechanisms of
The Tubular Web RBS connection (TW-RBS)

To evaluate the axial resistance tubular web in the reduced region and compare it with the axial resistance of a flat web, a cylindrical bar with the depth of the unit is considered. According to Fig. 1, the ultimate condition of a cylindrical bar under the effect of *P* makes four hinges at the end points and the center point of the circular. Free body diagram of a quarter segments can be considered due to establishment of symmetry. Accordingly, by writing the moment balance equation at a plastic joint, P_{corr} force can be obtained as follows

$$P_{corr} = \frac{8M_{pc}}{D} = \frac{8\frac{t_c^2}{4}F_y}{D} = \frac{2t_c^2 F_y}{D} \quad (1)$$

By taking the same height and letting $A_f = t_f$ for flat sheet we have

$$P_{falt} = A_f F_y = t_f F_y \quad (2)$$

Measurement of the impact on the resistance properties of tubular accordion web and a comparison between the tube resistance and flat web, Strength Degradation Factor (SDF) can be calculated as follows

$$SDF = 1 - \frac{P_{corr}}{P_{flat}} = 1 - \frac{2\left(\frac{t_c}{t_f}\right)^2}{\left(\frac{D}{t_f}\right)} \quad (3)$$

Based on the equation above, SDF is a function of pipe diameter ratio to flat web and tube thickness ratio to flat web.

Beam plastic moment in the corrugated area can be written as a function of axial resistance P_{flat} or P_{corr}. Letting $p(y) = -p$ for negative values of *y* and $p(y) = p$ for positive values of y in the web plastic state and also the cross section is symmetric about the neutral axis, plastic moment is calculated as follows

$$M = \frac{Ph^2}{4} \quad (4)$$

In this case, *p* is the axial strength and can be replaced by P_{corr} or P_{flat}. Because the plastic moment of web section is equal to $Z_{web}F_y$, then modulus of the plastic portion of web can be calculated as follows

$$M = \frac{Ph^2}{4} = Z_{web} F_y \quad (5)$$

$$Z_{web} = \frac{Ph^2}{4F_y} \quad (6)$$

Since the plastic modulus calculated by the contribution of web directly depends on the inside axial strength, the ratio of the plastic modulus of the tubular web to plastic modulus of the flat web, is P_{corr}/P_{flat} proportionally. In other words, the reduction factor of web plastic modulus is equal to SDF.

According to the results, the plastic modulus of the I-shaped beam along the tubular area can be calculated as follows

$$Z_{AWS} = Z_{flange} + (1 - SDF)Z_{web}^{flat} \quad (7)$$

Appendix 2
Controlling beam shear in plastic hinge region
(Tubular web region)

In corrugated sheets, shear buckling is controlled by interaction of buckling mode obtained from interaction of local and global buckling modes. Elastic local buckling shear stress can be calculated using Eq. (1) (Eldib 2009)

$$\tau_{cr,l}^e = k_1 \frac{\pi^2 E}{12(1 - v^2)}\left(\frac{t_w}{\omega}\right)^2 \quad (1)$$

In Eq. (1), *E* is the Young elastic modulus; *v* is the Poisson ratio, and ω is the maximum value of horizontal width (*a*) and diagonal width (*c*) of corrugated sheet (Fig. 1); t_w is the thickness of corrugated sheet; the local shear buckling coefficient k_1 is defined as follows (Eldib 2009). In Eq. (2), h_w is height of the corrugated web sheet

$$k_l = 5.34 + 4\left(\frac{\omega}{h_w}\right)^2 \quad (2)$$

Global buckling of corrugated sheet is calculated based on stability equations as follows (Eldib 2009).

$$\tau_{cr,G}^e = k_G \frac{\pi^2 E}{12(1 - v^2)}\left(\frac{t_w}{h_w}\right)^2 \quad (3)$$

General shear buckling coefficient k_G is defined as follows (Eldib 2009)

$$k_G = \frac{36\beta}{\pi^2\sqrt{\eta}}\left[2\left(\left(\frac{d}{t_\omega}\right)^2 + 1\right)(1 - v^2)\right]^{3/4} \quad (4)$$

Where, β is 1 and 1.9 for the simple and rigid edge connections, respectively; η defines length reduction factor which is calculated through $(a + b) / (a + c)$, d is the depth of corrugated sheet and *v* is assumed to be 0.3 in this study.

The equation for interaction shear buckling strength which was proposed by Eldib can be used for unusual corrugated sheets such as arcs (Eldib 2004). This equation was proposed based on Pachoumis's experimental study on 40 trapezoidal sheets (Hamilton 1993).

$$\left(\frac{1}{\tau_{cr,l}}\right)^n = \left(\frac{1}{\tau_{cr,B}}\right)^n + \left(\frac{1}{\tau_y}\right)^n \quad (5)$$

Where, value of *n* is 4 for local buckling and 1.5 for general buckling. Also $\tau_{cr,B}^e$ is the minimum value of localized and general shear buckling strength.